Measurement 243 (2025) 116334

Contents lists available at ScienceDirect

Measurement

journal homepage: www.elsevier.com/locate/measurement

Performance evaluation of marker tracking method for rotational speed measurement of wind turbine blades

Yi-Hsiang Liao [a], Lijuan Wang [a,*], Yong Yan [b]

[a] School of Engineering, University of Kent, Canterbury CT2 7NT, United Kingdom
[b] Hangzhou International Innovation Institute, Beihang University, Hangzhou 311115, China

ARTICLE INFO

Keywords:
Wind turbine blades
Instantaneous rotational speed measurement
Marker tracking
Image correlation

ABSTRACT

Rotational speed is one of the most important operating parameters of wind turbines. It is not only related to the power output but also the operating status of mechanical parts. To measure the rotational speed of wind turbine blades, image processing methods demonstrate the advantages of non-contact measurement and low maintenance requirements. However, it is still challenging to achieve instantaneous rotational speed with high accuracy. In this paper, a new marker tracking method is proposed and implemented to measure the instantaneous rotational speed of wind turbine blades. Experiments were conducted on a wind turbine test rig with different camera settings, camera positions, and lighting conditions to assess the performance of the proposed method. Results show that the maker tracking method achieves a relative error mostly within ±0.5 % and a normalised standard deviation below 0.35 % with the typical speed range of wind turbine blades from 5 rpm to 30 rpm. Compared with the existing image correlation and frequency analysis method, the maker tracking method produces accurate measurement results and faster response.

1. Introduction

As more and more countries shift from traditional energy sources to renewable energy, wind turbines are starting to play a major role in the grid. This higher demand has resulted in wind turbine manufacturers making larger wind turbines to improve their efficiency as well as their energy output. However, larger wind turbines pose a challenge to operation and maintenance. It is particularly challenging to monitor the structural health of wind turbine blades due to the vast and complex surfaces to inspect. Several measurable properties are useful for monitoring the structural health of a wind turbine. One of the important properties to monitor is the rotational speed of wind turbine blades. This is because a sudden change in rotational speed indicates possible defects such as ice accretion on the blades or damage in the transmission system.

Currently, the instantaneous angular speed (IAS) of a wind turbine's low-speed shaft is measured by using various angular sampling techniques. Typically, this is done by counting the pulses generated by the change in the magnetic field by placing a giant magnetoresistive sensor (GMR) near a geared wheel [1,2]. Although it is able to limit the measurement error within ±1.0° and an angle resolution of ±0.3°, it reflects little external information about the wind turbine blades. Several methods have addressed this using wireless inertial measuring units (IMUs) [3] mounted inside the blade near the root, or Doppler radars [4,5]. Although these methods can identify extra information such as edgewise and flapwise vibration displacement and fracture, it is challenging to determine the location of these faults.

With new advances in image processing, several imaging approaches have been proposed to measure rotational speed. One of them is to track the changes between frames using sparse optical flow and then project the changes onto the cylindrical coordinate system to find the rotation angle [6]. Sparse optical flow provides a way to track objects without any markers but requires the object to have texture (e.g. corners and edges) to track, which is not suitable for wind turbine blades due to them being smooth. Another method analyses the change in variance of a small region on the shaft to get the rotational speed [7]. The authors measured a motor at 1500 rpm with a camera recording at 125 fps. However, the change in variance is only visible on cylindrical objects so it is also unsuitable for wind turbines. Correlation can also be used to record the change in similarity and, when combined with frequency analysis techniques, can measure rotational speed ranging from 100 rpm to 3000 rpm [8,9]. The other family of methods uses marker to generate features for tracking. One of these methods uses Speeded Up Robust

* Corresponding author.
E-mail address: L.Wang@kent.ac.uk (L. Wang).

https://doi.org/10.1016/j.measurement.2024.116334
Received 7 August 2024; Received in revised form 1 November 2024; Accepted 27 November 2024
Available online 28 November 2024

Features (SURF) feature detector to track the random pattern on the shaft between frames [10]. This method was able to achieve relative errors below 3 % when measuring speeds from 602 rpm to 1466 rpm with a high-speed camera filming at 800 fps. Unfortunately, due to the high computation cost of SURF, a typical capture of 600 frames will require 10 s of processing time. Zhong et al. [11] proposed a novel method based on the analysis of fringe patterns on the shaft. This method can measure not only the rotational speed but also the axial vibration but again only limited to shaft-like objects. Another method also measures the rotational speed of propellers from rolling shutter artefacts [12]. However, this method relies on good-quality segmentation, which is challenging in outdoor scenarios.

Image processing methods have also been used to measure the rotational speed of wind turbine blades. Natili et al. [13] calculated the similarity between the reference frame and subsequent frames with Pearson correlation and then used short-time Fourier transform (STFT) to get the rotational speed of wind turbines. Experiments were conducted to measure rotational speed on smaller wind turbines with rotational speed in the range of 750 rpm to 1500 rpm as well as large wind turbines with a rotational speed of 27 rpm. However, the performance of the correlation method for large wind turbines which normally operate ranging between 5 rpm to 50 rpm is unclear. In our preliminary study [14], a simple marker tracking method with a blob detector has been proposed for rotational speed measurement of wind turbines. The performance of this simple marker tracking method has been evaluated in comparison with the method used in reference [13] on a simulated wind turbine model with the speed range between 5 rpm and 30 rpm. The results have demonstrated that the relative error of the simple marker tracking method is mostly within ± 0.5 %, while the correlation method requires a large window size to measure at lower rotational speeds to ensure accuracy, thus resulting in longer response time for lower speed measurement. Recently, a machine learning-based tracking system with two cameras was proposed [15], which uses the extended Kalman filter (EKF) to estimate the angular speed of the wind turbine blades for the purpose of position prediction. However, the accuracy of angular speed measurement was not analysed in the experimental results.

This paper proposes a new marker tracking method with a square marker detector to improve the accuracy and response time in rotational speed measurement of wind turbine blades which operate at lower speeds. In the meantime, the computational process is simplified compared with reference [14] to improve efficiency. Unlike other marker tracking methods that use complex markers or random patterns, the square marker detector does not rely on extra transformations or estimations, making it efficient and deterministic. Moreover, the proposed method also allows tracking of any rotating objects with markers applied perpendicular to the rotation axis, making it suitable for wind turbine applications. In addition, the proposed method provides faster response in comparison to time-dependent methods like the correlation-based methods. The main contributions of the work are summarized as follows:

(1) To improve the accuracy of marker tracking on wind turbine blades, a new square marker detector algorithm is applied in this paper. The processes of marker matching and angle calculation are combined for the purpose of computational efficiency.
(2) To understand the effects of camera setting, camera position and light condition on the performance of the measurement system, experimental studies are conducted on a purpose-built wind turbine test rig.
(3) Performance comparison between the proposed marker tracking method and the image correlation with frequency analysis method is undertaken to evaluate their accuracy, stability and response time.

The paper is organised into five sections. It starts with the introduction and background information on wind turbine blade rotational speed measurement. Section two describes the measurement principle and methodology. The experimental setup used to collect our data is then shown in section three. The results of the experiments are presented in section four along with discussions on the effects of environmental conditions and the comparison with the state-of-the-art correlation method. Finally, a conclusion is drawn from the results and future work is presented.

2. Measurement principle

The overview of the marker tracking method is shown in Fig. 1. The sequence of frames is captured by the camera pointing to the wind turbine blades. One way to accomplish this in practical scenarios is to attach a camera to a drone. The captured frame sequence is followed by a square marker detector, where the positions of the three markers in the individual frames are determined. Square markers were used due to their unique geometric property of equal width and height, which stands out compared to typical shapes found on wind turbines. Based on the marker positions, the centre of rotation is calculated, and adjacent marker positions are matched using their angular distance. The angular velocity can then be calculated using the angular distance and the frame rate. Finally, angular velocity is converted to RPM (Revolutions Per Minutes).

The flowchart for the square marker detector is shown in Fig. 2 followed by a step-by-step result shown in Fig. 3. The image is first converted to grayscale and enhanced by calculating the mean and standard deviation of the histogram and setting pixel values above three standard deviations to zero, as shown in Eq. (1).

$$f(x) = \begin{cases} 0, & x > \mu + 3\sigma \\ x, & otherwise \end{cases} \tag{1}$$

where x is the pixel intensity, μ is the mean of the grayscale value, and σ is the standard deviation.

The enhanced image is then inverted, which changes the distribution of the histogram and further improves the segmentation of the markers. The markers are segmented using 0.7 of the maximum grayscale value. This parameter can be tuned to accommodate different image contrasts or light conditions. Following the segmentation, the binary image goes through contour analysis, and the contours are filtered by its area to exclude some patches that are too large or invalid. It should be noted that, instead of using a fixed pixel area, the proportion of patch area to total area is used to make the algorithm scale invariant. After ruling out patches with the wrong size, the rotated bounding box is calculated and sorted by squareness as defined in Eq. (2) to find the patches that are closest to a square. The closer the calculated squareness is to 0, the closer it is to a square.

$$squareness = \left| 1 - \frac{A}{max(w_{bbox}, h_{bbox})^2} \right| \tag{2}$$

where w_{bbox} is the width of the bounding box, h_{bbox} is the height of the bounding box, A is the area of the patch.

A detected square marker is used to demonstrate the squareness evaluation method in Fig. 4. The blue section is the area for the nominator and the yellow patch is the denominator part. With the w_{bbox} of 90 pixels, h_{bbox} of 94 pixels and A of 8158 pixels, the squareness is of the patch is calculated as 0.076. The reason behind using the max operator is to eliminate long rectangles. Very long patches (e.g., the shadow of the rails in a captured image) will have a similar patch area and bounding box area.

Once the square markers are detected, the centre of rotation is calculated by finding moments using the 3 marker centres. Then, three vectors were formed (shown in Fig. 5) by subtracting the coordinates of the marker centres with the centre of rotation of each frame. Since the markers are identical, the only way to distinguish them is by their

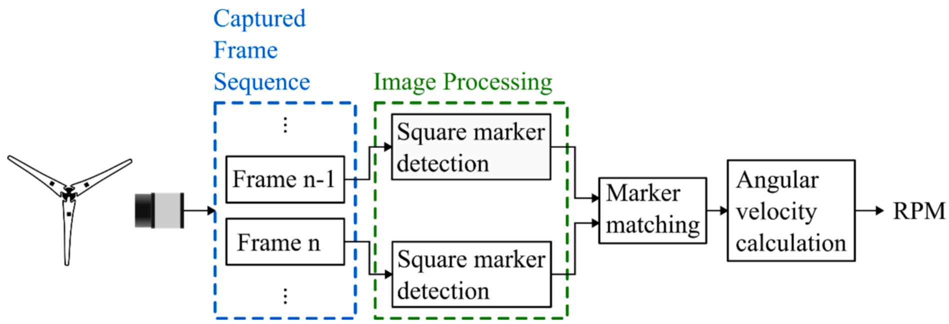

Fig. 1. Overview of the proposed marker tracking method.

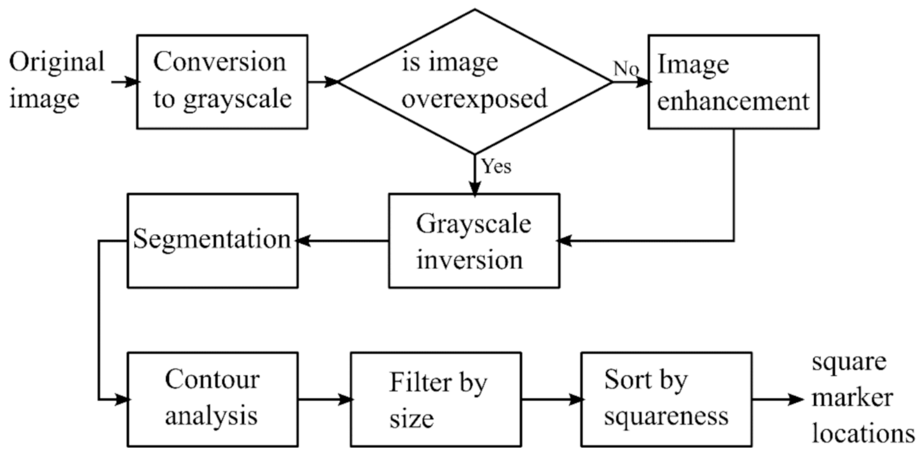

Fig. 2. Flowchart for preprocessing and marker detection.

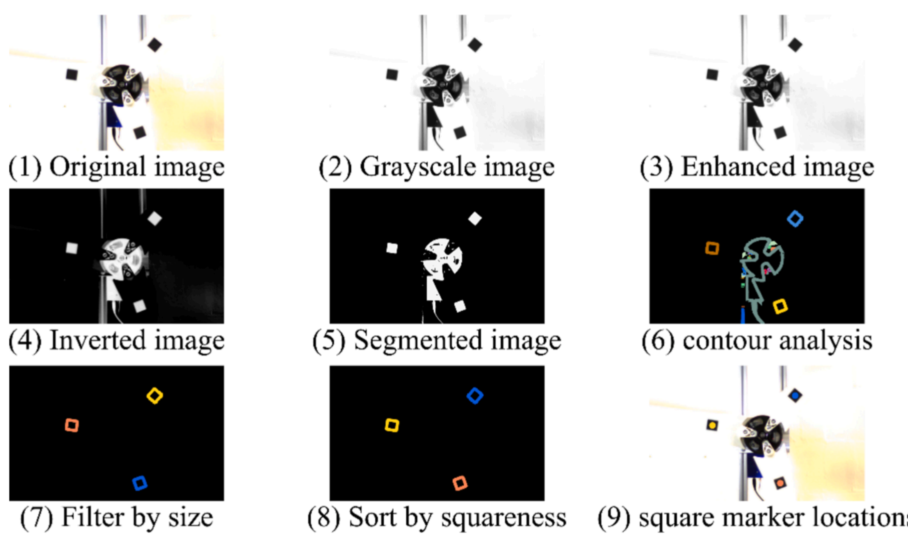

Fig. 3. Processing steps of the square marker detector.

distance between frames. In this paper, cosine distance as defined in Eq. (3) is used.

$$\text{cosine distance} = 1 - \cos\frac{\overrightarrow{v_{(n-1),i}} \cdot \overrightarrow{v_{n,i}}}{\left|\overrightarrow{v_{(n-1),i}}\right|\left|\overrightarrow{v_{n,i}}\right|} \quad (3)$$

where $\overrightarrow{v_{(n-1),i}}$ are the vectors from the *(n-1)*th frame (previous frame), $\overrightarrow{v_{n,i}}$ are the vectors from the *n*th frame (current frame), and *i* is the index of the marker.

After calculating all combinations of vector distances, the smallest three are selected and indices are paired. In addition, cosine distance doubles as a way to calculate the rotation angle (θ_i) between frames. With the information of the rotation angle and the camera's frame rate, the angular velocity can be derived and converted to RPM according to Equation (4).

$$RPM = \frac{10}{\pi} \cdot \sum_{i=1}^{3} \theta_i \cdot f_s \quad (4)$$

where f_s is the camera frame rate, θ_i is the rotation angle of each

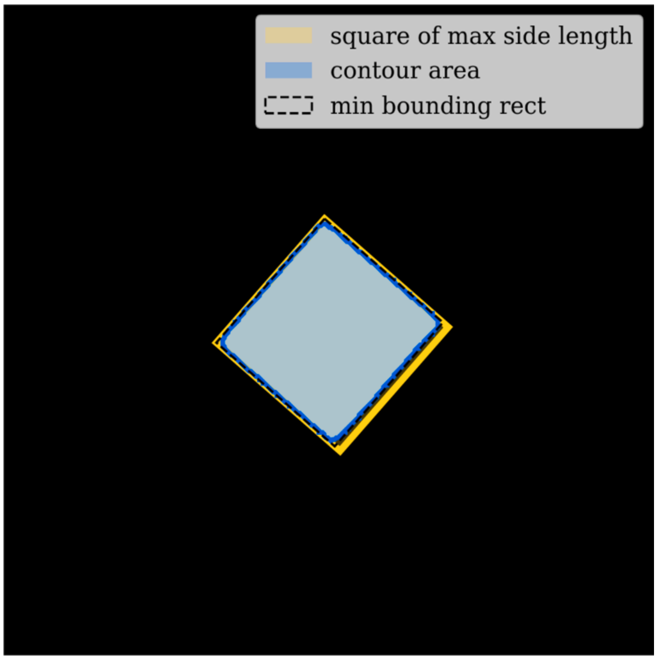

Fig. 4. Showcase of squareness evaluation on one of the detected markers.

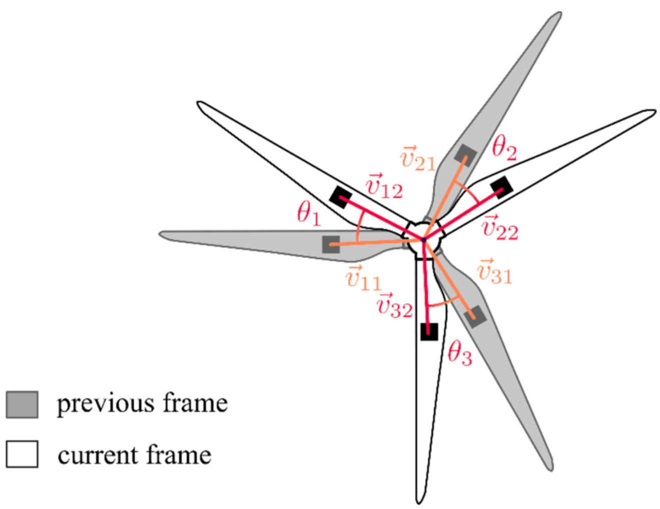

Fig. 5. Illustration of marker matching and angle calculation strategy.

blade between frames.

3. Experimental setup

Experiments were conducted on a test rig shown in Fig. 6. The test rig is a modified wind turbine with three blades that are 600 mm in length. The blades are controlled by a stepper motor to rotate from 5 rpm to 30 rpm, which is the typical operation range in wind farms.

The camera (UEYE U3-3060CP-C-HQ Rev.2) used in this study is a camera with a maximum framerate of 166 fps at a resolution of 1936×1216, and a gain that ranges from 0 % to 100 %. Additionally, the camera is paired with a 25 mm lens with an aperture $f/2.8$. The light panels are there to change the light conditions during experiments. The commercial laser tachometer (PLT200) is used as a reference to our measurement with an accuracy of ±0.01 %, and it is calibrated by the National Institute of Standards and Technology (NIST). This ensures measurements made by the system in this study to be traceable. A Retroreflective sticker was placed behind a blade to prevent interference from the laser when the camera was recording. Whenever the tachometer detects a reflected laser, it outputs a pulse. Pulses were acquired by the data acquisition unit (NI-USB6341) and sent to the laptop for processing.

During experimental tests, the camera is recording at 30 frames per second (fps) with a resolution of 1936×1216. To provide stable image captures, the camera is mounted on a tripod. The distance between the camera and the centre of rotation is set to 1.8 m. The black square markers are 35 mm on both sides and placed 150 mm away from the centre. This position ensures all three markers are visible in a full rotation. Fig. 7 shows a typical captured frame with a bit of motion blur on markers. The further away the markers from the centre of rotation, the more motion blur on them due to the higher linear velocity of blade tips. This is the other reason to put the markers close to the centre.

Experimental tests are designed to assess the performance of the proposed speed measurement method under different conditions. As shown in Table 1, three different exposure (16 ms, 19 ms, 24 ms) and gain (30 %, 50 %, 70 %) combinations were firstly tested to evaluate the effects of camera settings on the measured results. In test II, with the fixed camera setting, the yaw angle of the camera was changed from 0°, 15°, to 30° to investigate the effects of camera position on the measured results. Subsequently, two different lighting conditions (200 lx and 50 lx) were set to test the robustness of the proposed method. In test IV, the performance of marker tracking method and the image correlation and frequency analysis method were assessed under the same experimental conditions.

4. Results and discussion

During the experiments, the measured speed from the marker tracking method and the reference speed from the optical tachometer were recorded at the same time. Fig. 8 shows the typical measured results and reference when turbine blades were rotating at 15 rpm. Due to the fact that the tachometer only completes one measurement per rotation when the laser tachometer detects the retroreflective marker whereas the proposed marker tracking method produces one measured result per frame, the reference has far fewer speed samples. Compared with the reference, the measured results are very close to 15 rpm, mostly varying between 14.95 rpm to 15.1 rpm.

4.1. Effects of camera setting

To evaluate the effect of the camera setting for measuring the rotational speed of wind turbine blades, the camera was set with different exposure (16 ms, 19 ms, 24 ms) and gain (30 %, 50 %, and 70 %) values. During the experimental tests, the illumination remained at 200 lx, and the wind turbine was controlled to rotate at constant speeds between 5 rpm to 30 rpm. For each exposure and gain combination, the relative error and normalised standard deviation of the measured speeds from the marker tracking method are shown in Fig. 9. It demonstrates that the proposed method performs well in general, with a relative error between −1.3 % and 0.75 % and a normalised standard deviation of less than 0.35 % for different camera settings. However, larger relative error and higher standard deviation are usually seen at the speed of 5 rpm. This is because lower speeds generate smaller changes in angle, resulting in higher floating-point errors during arithmetic operations. As rotational speed increases, a smaller difference in relative error suggests less effect of exposure and gain on the measured results. Since the exposure of 19 ms and gain of 70 % yields lower relative error and standard deviation, particularly at a lower speed, this is the camera setting of choice in tests II – IV.

4.2. Effects of camera position

To assess the performance of the proposed method under different camera positions, the camera was set to different yaw angles (0°, 15°,

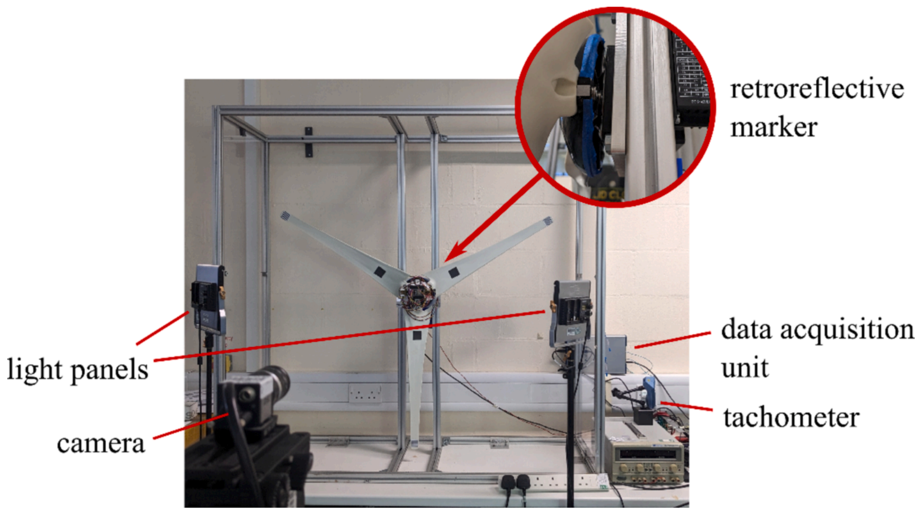

Fig. 6. Experimental test rig and measurement system.

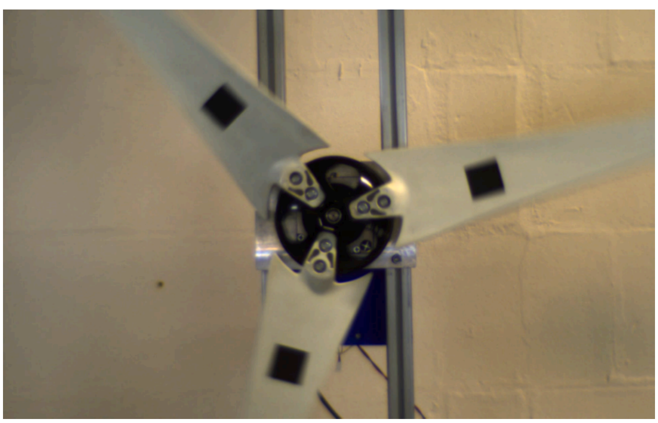

Fig. 7. Typical captured frame from the camera at 15 rpm with 200 lx environmental lighting.

30°), where 0° refers to the camera positioned perpendicular to the rotational plane. Due to the point symmetry property of wind turbine blades with respect to the hub, the pitch angle will have the same effect as yaw angles on the measured results. The relative error and normalised standard deviation of measured rotational speed in different yaw angles are shown in Fig. 10. It is obvious that relatively higher errors are produced from the yaw angles of 15° and 30°, mostly within ±1.5 % over the rotational speed range. In addition, it is evident that the normalised standard deviation increases with yaw angle for a constant rotational speed. This is because a larger yaw angle changes the perspective, and the centroid of the markers is no longer the centre of rotation.

4.3. Effects of lighting condition

With the fixed camera setting (exposure of 19 ms and 70 % gain) and camera position (0° of both yaw and pitch), the proposed measurement method was evaluated under different lighting conditions. The blades were rotating from 5 rpm to 30 rpm with two illuminances – 200 lx and 50 lx. The relative error and normalised standard deviation of the measured speed are shown in Fig. 11. For the illuminance of 200 lx, the relative error is between −0.95 % and 0.75 %. However, the normalised standard deviation decreases from 0.35 % at 5 rpm to 0.12 % at 10 rpm and stays within 0.05 % for higher rotational speeds. The same trend is depicted for results from the 50 lx condition, which indicates that rotational speed measurements become more stable as speed increases. Comparing the results from the two light conditions, it can be seen that the normalised standard deviation at each speed with an illuminance of 50 lx is slightly higher than that with an illuminance of 200 lx. This is due to the higher camera noise and lower contrast at low light conditions, which affects the ability to accurately determine the position of square markers.

4.4. Comparison between different algorithms

An experimental study was carried out to compare the performance of the proposed marker tracking method with the existing method – image correlation with frequency analysis for instantaneous rotational speed measurement. As chirp-Z transform (CZT) has been demonstrated better performance in determination of periodicity with limited sampling time than the short-time Fourier transform in [9], the image correlation with CZT method is applied in this study for comparison. This image correlation with CZT method aims to obtain the similarity level firstly by calculating the correlation coefficient between a reference frame and all consecutive frames. The generated time-series signal indicating similarity level is then analysed using CZT to get the rotational frequency.

The two methods were implemented and tested on the wind turbine test rig to obtain the rotational speed of blades. The typical measurement results are shown in Fig. 12. As a window of 510 samples is required for rotational frequency analysis to ensure the accuracy of measurement, only 40 measured results are obtained throughout the period of 30 s from the image correlation with CZT method. This is also

Table 1
Test Matrix.

No	Rotational speed (rpm)	Camera exposure (ms)	Camera gain (%)	Camera yaw (°)	Illumination (lux)	Algorithm
I	5, 10, 15, 20, 25, 30	16/19/24	30/50/70	0	200	marker tracking
II	5, 10, 15, 20, 25, 30	19	70	0/15/30	200	marker tracking
III	5, 10, 15, 20, 25, 30	19	70	0	200/50	marker tracking
IV	5, 10, 15, 20, 25, 30	19	70	0	200	marker tracking, image correlation with frequency analysis

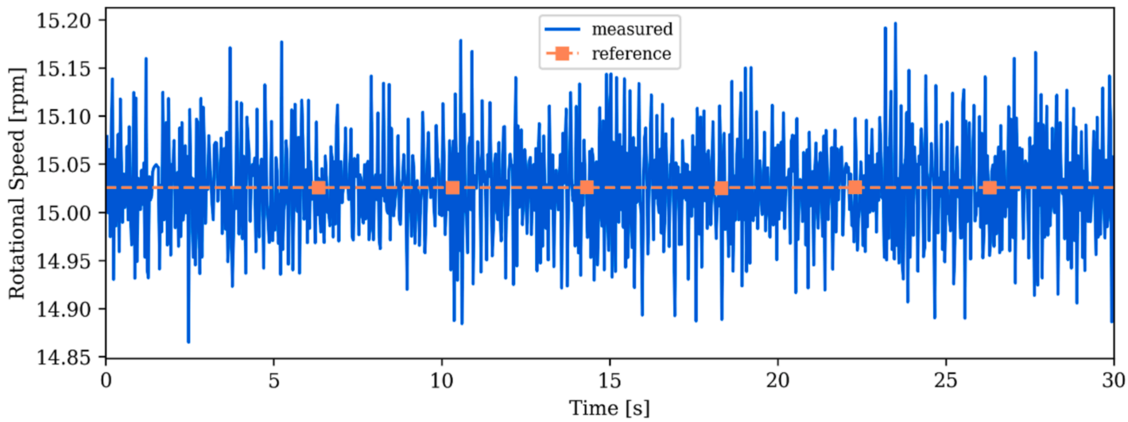

Fig. 8. Typical measurement results at a rotational speed of 15 rpm.

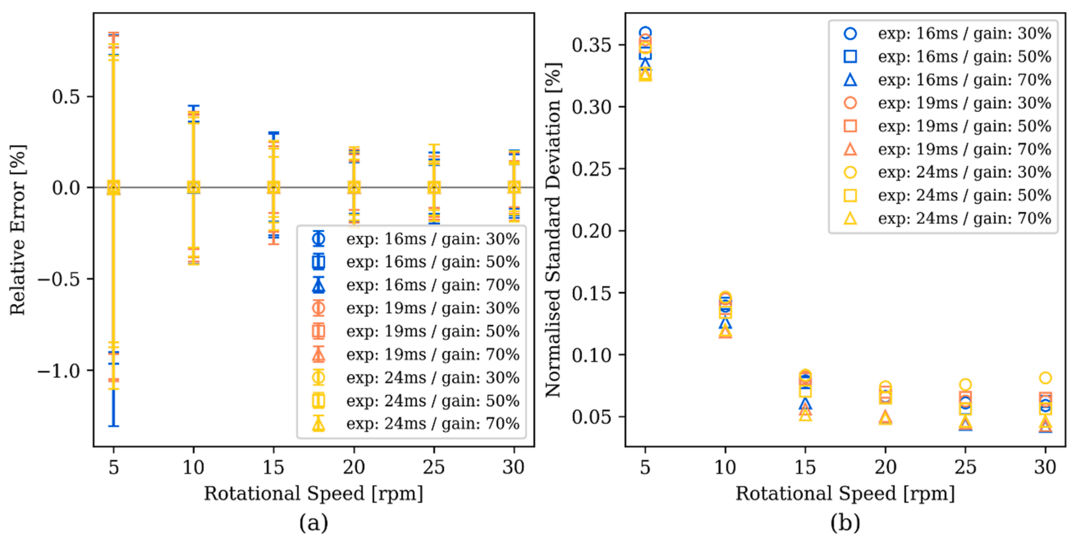

Fig. 9. Relative error (a) and normalised standard deviation (b) of measured rotational speed with different camera exposure and gain combinations.

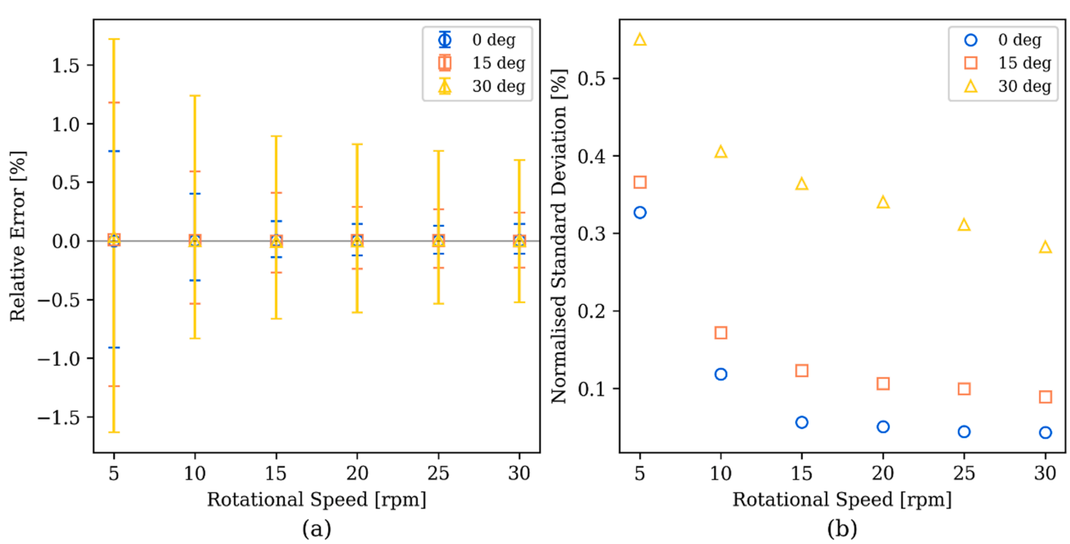

Fig. 10. Relative error (a) and normalised standard deviation (b) of measured rotational speed in different yaw angles.

the reason why there is a long starting time of more than 8 s for this method. However, the marker tracking method provides instantaneous response and hence more measured results. As shown in Fig. 13, with optimal camera setting, camera position and lighting condition, the marker tracking method produces a relative error between −0.95 % and 0.75 % in all cases with a normalised standard deviation no greater than

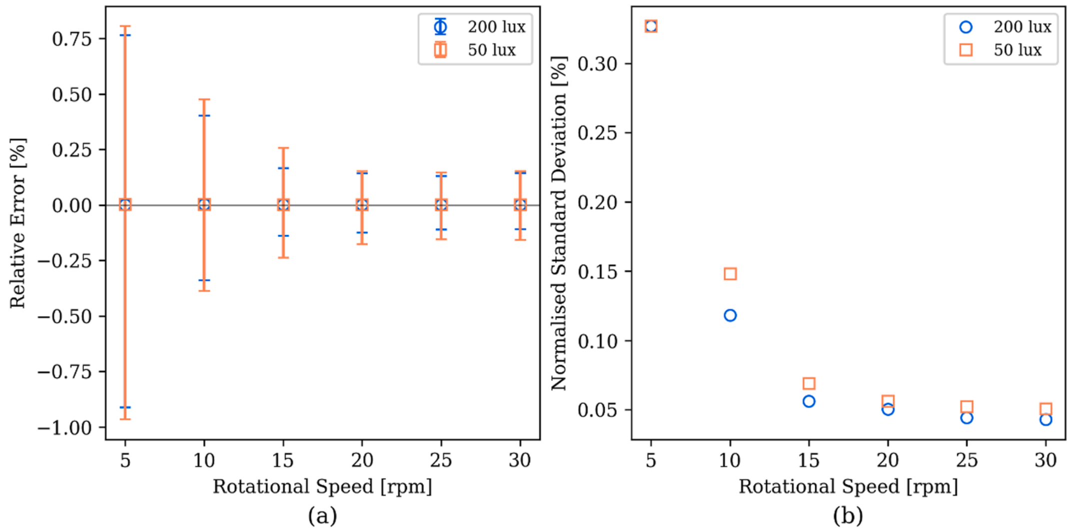

Fig. 11. Relative error (a) and normalised standard deviation (b) of measured rotational speed with different illuminances.

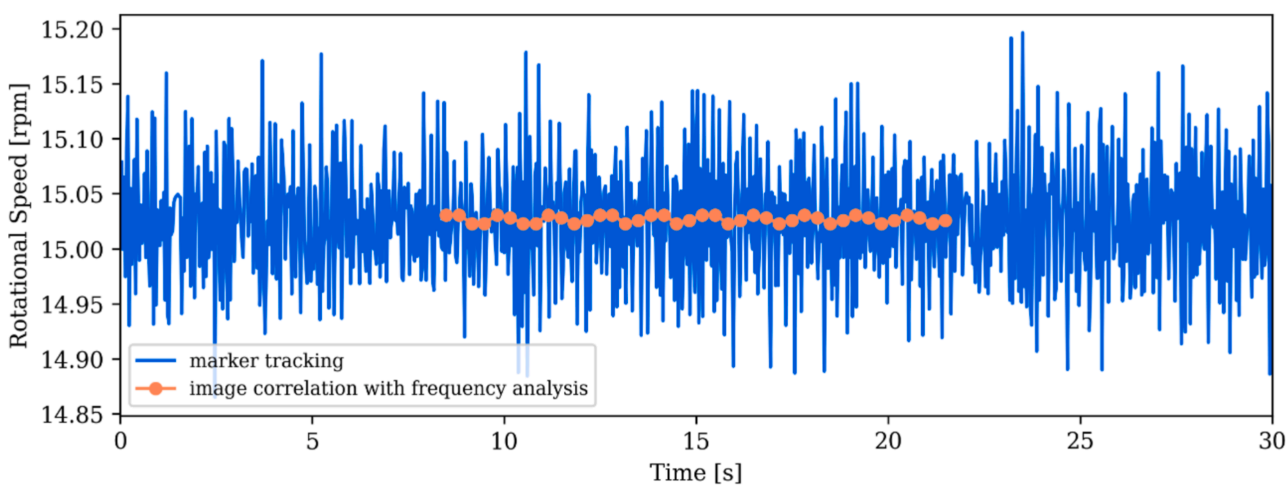

Fig. 12. Typical measurement results of 15 rpm with different algorithms.

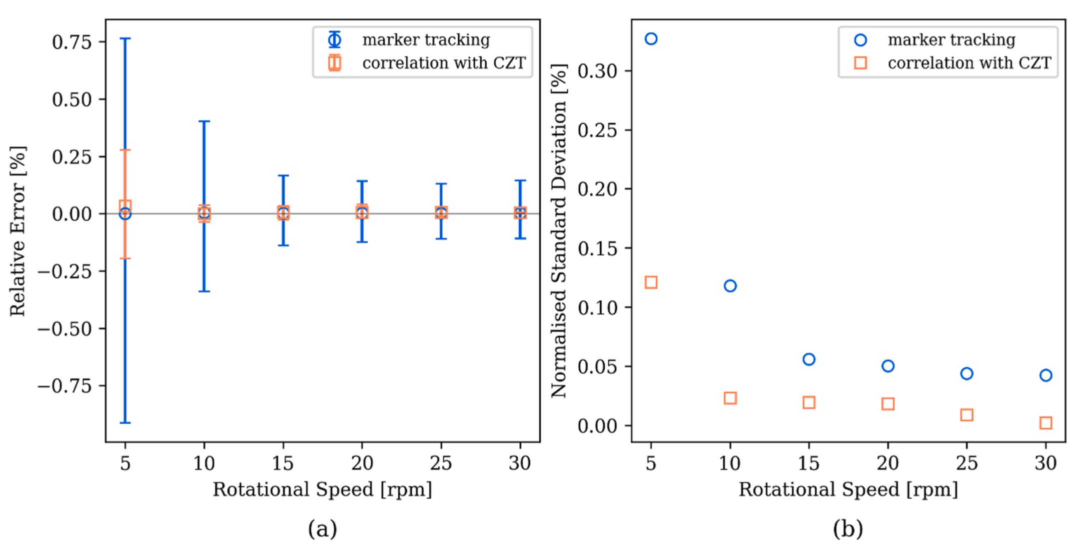

Fig. 13. Relative error (a) and normalised standard deviation (b) of rotational speeds between different algorithms.

0.35 %. However, the marker tracking method produces a slightly higher error than the correlation with CZT method at lower speeds. The error of the marker tracking method is mainly caused by the smaller angle change at lower speed which results in relatively higher floating-point error in the determination of rotational angle. However, for the correlation with CZT method, the rotational speed is measured by the determination of the rotational frequency of the periodic signal within the window, not the rotational angle. Therefore, the performance of the correlation with CZT method is less affected at lower speeds. It should be noted that the marker tracking method produces a faster response than the image correlation with the frequency analysis method and is thus more suitable for instantaneous speed measurement scenarios.

5. Conclusion

In this paper, a new square marker tracking method was proposed to measure the rotational speed of wind turbine blades. Through analysing the measurements' relative error and normalised standard deviation of various exposure and gain combinations, it has been found that exposure of 19 ms and gain of 70 % performed better than other camera settings at lower speeds. The effect of camera parameters slowly decreases as the rotational rises. Experimental results have suggested that higher yaw angle and weak illuminance mainly affect the stability of the measurement with increased standard deviation. With the camera exposure of 19 ms and gain of 70 %, yaw angle of 0° and illuminance of 200 lx the marker tracking method has achieved a relative error mostly within ± 0.5 % with a normalised standard deviation no greater than 0.35 %. In comparison with the image correlation with CZT method, the maker tracking method produces accurate results with faster responses. This demonstrates the feasibility of measuring the instantaneous rotational speed of wind turbine blades by tracking a simple square marker under laboratory conditions with the chosen camera parameters, camera positions, and environment brightness. In general, this marker tracking method can be used to determine the rotational speed of any rotating object by applying one or more markers as long as there is enough space for a camera to capture the markers in a series of frames. The developed square marker detector and marker matching algorithms are also applicable to other applications of rotational speed measurement.

The limitation of the proposed method is its inability to function when some of the marker is obscured. This can happen due to perspective changes (acute camera angles) or simply uneven lighting. However, this can be solved by a fallback method that estimates the centre of rotation by calculating the angle of the detected square markers. Overall, the proposed marker tracking method can provide a direct and effective way to measure the rotational speed of a wind turbine. Field tests will be conducted in the future to evaluate the performance of the proposed method in an outdoor setting. Further enhancements into the method such as the centre of rotation fallback will also be implemented to improve the robustness of this method.

CRediT authorship contribution statement

Yi-Hsiang Liao: Writing – original draft, Methodology, Formal analysis, Data curation. **Lijuan Wang:** Writing – review & editing, Supervision, Methodology, Conceptualization. **Yong Yan:** Writing – review & editing, Supervision, Methodology, Conceptualization.

Declaration of competing interest

The authors declare that they have no known competing financial interests or personal relationships that could have appeared to influence the work reported in this paper.

Data availability

Data will be made available on request.

References

[1] C. Giebeler, D.J. Adelerhof, A.E.T. Kuiper, J.B.A. van Zon, D. Oelgeschläger, G. Schulz, Robust GMR sensors for angle detection and rotation speed sensing, *Sens. Actuators Phys.* 91 (1) (2001) 16–20, https://doi.org/10.1016/S0924-4247(01)00510-6.

[2] S. Butzmann and R. Buchhold, "A new differential magnetoresistive gear wheel sensor with high suppression of external magnetic fields [automotive applications]." In *2004 IEEE SENSORS*. Oct. 2004. pp. 16–19. vol.1. doi: 10.1109/ICSENS.2004.1426088.

[3] F. Berkemeyer, W. Lang, Wireless Inertial Measurements on Wind Turbine Rotor Blades, *IEEE Sens. J.* 21 (24) (2021) 27938–27946, https://doi.org/10.1109/JSEN.2021.3122952.

[4] H. Zhao, G. Chen, H. Hong, X. Zhu, Remote Structural Health Monitoring for Industrial Wind Turbines Using Short-Range Doppler Radar, *IEEE Trans. Instrum. Meas.* 70 (2021) 1–9, https://doi.org/10.1109/TIM.2021.3053959.

[5] Y. Choi, Y. Kim, and I.-S. Choi. "Measurement of the rotational speed of industrial wind turbine blades using a low cost 24GHz Doppler radar." In *2021 15th European Conference on Antennas and Propagation (EuCAP)*. Mar. 2021. pp. 1–5. doi: 10.23919/EuCAP51087.2021.9411170.

[6] Y. Zhang, G. Cao, J. Cao, Target-less approach of wire rope rotation measurement, *Measurement* 221 (2023) 113489, https://doi.org/10.1016/j.measurement.2023.113489.

[7] F. J. T. E. Ferreira, A. F. F. Duarte, and F. J. P. Lopes. "Experimental Evaluation of a Novel Webcam-Based Tachometer for In-Situ Rotational Speed Measurement." In *2020 IEEE International Conference on Industrial Technology (ICIT)*. Feb. 2020. pp. 917–924. doi: 10.1109/ICIT45562.2020.9067295.

[8] T. Wang, Y. Yan, L. Wang, Y. Hu, Rotational Speed Measurement Through Image Similarity Evaluation and Spectral Analysis, *IEEE Access* 6 (2018) 46718–46730, https://doi.org/10.1109/ACCESS.2018.2866479.

[9] T. Wang, Y. Yan, L. Wang, Y. Hu, S. Zhang, Instantaneous Rotational Speed Measurement Using Image Correlation and Periodicity Determination Algorithms, *IEEE Trans. Instrum. Meas.* 69 (6) (2020) 2924–2937, https://doi.org/10.1109/TIM.2019.2932154.

[10] X. Wang, J. Guo, S. Lu, C. Shen, Q. He, A computer-vision-based rotating speed estimation method for motor bearing fault diagnosis, *Meas. Sci. Technol.* 28 (6) (2017) 065012, https://doi.org/10.1088/1361-6501/aa650a.

[11] J. Zhong, et al., Vision-based system for simultaneous monitoring of shaft rotational speed and axial vibration using non-projection composite fringe pattern, *Mech. Syst. Signal Process.* 120 (2019) 765–776, https://doi.org/10.1016/j.ymssp.2018.11.006.

[12] Y. Zhao, Y. Li, S. Guo, T. Li, Measuring the Angular Velocity of a Propeller with Video Camera Using Electronic Rolling Shutter, *J. Sens.* 2018 (2018), https://doi.org/10.1155/2018/1037083 e1037083.

[13] F. Natili, F. Castellani, D. Astolfi, M. Becchetti, Video-Tachometer Methodology for Wind Turbine Rotor Speed Measurement, *Sensors* 20 (24) (2020) 7314, https://doi.org/10.3390/s20247314.

[14] Y.-H. Liao, L. Wang, and Y. Yan. "Instantaneous Rotational Speed Measurement of Wind Turbine Blades using a Marker-Tracking Method." in *2022 IEEE International Instrumentation and Measurement Technology Conference (I2MTC)*. May 2022. pp. 1–5. doi: 10.1109/I2MTC48687.2022.9806658.

[15] S. Dutta, S. Liu, J. Karigiannis, Y. T. Tan, C. B. Theurer, and G. Song. "Autonomous Wind-Turbine Blade Tracking Using A Dual-Camera System." In *2023 29th International Conference on Mechatronics and Machine Vision in Practice (M2VIP)*. Nov. 2023. pp. 1–6. doi: 10.1109/M2VIP58386.2023.10413412.